

A User-Friendly Code to Diagnose Chromospheric Plasmas

A. Asensio Ramos¹ and J. Trujillo Bueno^{1,2}

¹*Instituto de Astrofísica de Canarias, La Laguna, Spain*

²*Consejo Superior de Investigaciones Científicas, Spain*

Abstract. The physical interpretation of spectropolarimetric observations of lines of neutral helium, such as those of the 10830 Å multiplet, represents an excellent opportunity for investigating the magnetism of plasma structures in the solar chromosphere. Here we present a powerful forward modeling and inversion code that permits either to calculate the emergent intensity and polarization for any given magnetic field vector or to infer the dynamical and magnetic properties from the observed Stokes profiles. This diagnostic tool is based on the quantum theory of spectral line polarization, which self-consistently accounts for the Hanle and Zeeman effects in the most general case of the incomplete Paschen-Back effect regime. We also take into account radiative transfer effects. An efficient numerical scheme based on global optimization methods has been applied. Our Stokes inversion code permits a fast and reliable determination of the global minimum.

1. Introduction

The quality of spectropolarimetric observations of solar chromospheric plasmas is steadily increasing. However, in order to obtain reliable empirical information on the strength and geometry of the magnetic field vector we also need to develop and apply suitable diagnostic tools within the framework of the quantum theory of spectral line polarization (e.g., the recent monograph by Landi Degl’Innocenti & Landolfi 2004). In particular, the development of a forward modeling and inversion code of Stokes profiles is of great importance because it would facilitate the investigation of a variety of problems of great astrophysical interest. For such a diagnostic tool to be reliable, it has to include all the important physical mechanisms that induce spectral line polarization in stellar atmospheres (e.g., the recent review by Trujillo Bueno 2006). Not only the Zeeman effect, but also the atomic level polarization induced by anisotropic radiation pumping and its modification by the Hanle effect have to be taken into account. For a remarkable example of a pioneering work in this field see Landi Degl’Innocenti (1982).

One of the main motivations of our investigation has been to develop a robust but user-friendly computer program for facilitating the analysis of the polarization signals induced by the above-mentioned physical mechanisms in the spectral lines of the He I 10830 Å multiplet, which are sensitive to both the Zeeman effect and to the presence of atomic level polarization (Trujillo Bueno et al. 2002; Trujillo Bueno & Asensio Ramos 2007). Spectro-polarimetric observations of this multiplet have been carried out in a variety of plasma struc-

tures of the solar chromosphere and corona, such as sunspots (Harvey & Hall 1971; Rüedi et al. 1995; Centeno et al. 2006), coronal filaments (Lin et al. 1998; Trujillo Bueno et al. 2002), prominences (Trujillo Bueno et al. 2002; Merenda et al. 2006), emerging magnetic flux regions (Solanki et al. 2003; Lagg et al. 2004), chromospheric spicules (Trujillo Bueno et al. 2005), active region filaments (Martínez Pillet et al. 2007; in preparation) and flaring regions (Sasso et al. on p. 467 ff of these proceedings).

2. The Forward Modeling Option

The adopted atomic model includes the following five terms of the triplet system of HeI: $2s^3S$, $2p^3P$, $3s^3S$, $3s^3P$ and $3d^3D$. It has been concluded that this 11 J -levels model with 6 radiative transitions between the terms is enough for a satisfactory modeling of the polarization properties of the spectral lines of the HeI D_3 multiplet at 5876 Å (Bommier 1977; Landi Degl’Innocenti 1982), and it should be also a reasonable approximation for those of the HeI 10830 Å multiplet which result from transitions between the terms $2s^3S$ and $2p^3P$.

It is well-known that the HeI atom can be correctly described by the L-S coupling scheme (e.g., Condon & Shortley 1935). The different J -levels are grouped in terms with well defined values of the electronic angular momentum L and the spin S . The energy separation between the J -levels inside each term is very small in comparison with the energy difference between different terms. Therefore, in addition to the atomic polarization of each J -level (population imbalances and coherences between its magnetic substates), it turns out to be fundamental to allow for coherences between different J -levels pertaining to the same term. However, coherences between different J -levels pertaining to different terms can be safely neglected. In conclusion, we can describe the atom via the formalism of the multi-term atom (see Sections 7.5 and 7.6 of Landi Degl’Innocenti & Landolfi 2004).

The atomic level polarization is quantified by the multipole components, $\rho_Q^K(J, J')$, of the atomic density matrix (Landi Degl’Innocenti & Landolfi 2004). The number of real quantities required to describe the excitation state of our multi-term model atom is 405. The helium atoms are illuminated by the (given) anisotropic radiation field coming from the underlying solar photosphere (Pierce 2000), whose properties are quantified by two spherical tensors: J_0^0 and J_0^2 (see Eq. 5.164 in Landi Degl’Innocenti & Landolfi 2004). They describe the mean intensity and the “degree of anisotropy” of the radiation field, respectively. We also consider that a magnetic field \mathbf{B} is present, with strength B , inclination θ_B with respect to the local vertical and azimuth χ_B . The density matrix elements are obtained by solving the statistical equilibrium equations (see Section 7.6a of Landi Degl’Innocenti & Landolfi 2004), which take into account the effect of the radiative transitions in the presence of the Zeeman splittings produced by the assumed magnetic field vector.

Once the elements of the atomic density matrix are known, the coefficients of the emission vector and of the propagation matrix of the Stokes-vector transfer equation can be directly calculated (see Section 7.6b of Landi Degl’Innocenti & Landolfi 2004). The next step is to compute the emergent Stokes profiles by solving the Stokes-vector transfer equation. To this aim, our code includes several options.

The simplest one assumes that the emergent Stokes profiles are simply proportional to the corresponding emissivity. This optically-thin case is representative of the conditions found in some prominences. The second option assumes that the HeI atoms are located in a slab of constant physical properties characterized by a non-negligible optical depth $\Delta\tau$ and that magneto-optical effects are negligible (see Trujillo Bueno et al. 2005 for the analytical expressions of the emergent Stokes profiles). Finally, the most general radiative transfer option is accomplished by using the DELOPAR method (Trujillo Bueno 2003).

Following the previously described approach, we have developed an efficient computer program that we have combined with an easy-to-use interactive front-end. It allows to interactively select the physical effects to be taken into account, thus helping to achieve a fast and reliable investigation of the influence of various physical parameters on the emergent Stokes parameters (for a first application, see Trujillo Bueno & Asensio Ramos 2007). For instance, our code allows to include or discard the effect of the magneto-optical terms and/or stimulated emission processes. Furthermore, it is possible to carry out the forward modeling including or neglecting the presence of atomic polarization. When atomic polarization is not taken into account, the problem reduces to the simplified case of the Zeeman effect, but with the positions and strengths of the σ and π components calculated within the framework of the incomplete Paschen-Back effect theory. This is important for the HeI 10830 Å multiplet because the linear Zeeman effect theory underestimates the inferred magnetic field strength (Socas-Navarro et al. 2004). In the absence of atomic level polarization, the emergent spectral line radiation is polarized due to the non-zero magnetic splitting produced by the presence of the magnetic field. For completeness, the Milne-Eddington solution of the radiative transfer equation can also be used in this case. By default, the total Hamiltonian (including the fine structure and magnetic contributions) is diagonalized numerically. However, our code also permits to calculate the emergent Stokes profiles assuming the linear Zeeman regime, which is useful in order to compare with those calculated within the framework of incomplete Paschen-Back theory.

3. The Stokes Inversion Option

The previously described forward modeling code has been also combined with a robust inversion scheme. The inversion algorithm is based on the minimization of a merit function that describes how well our model reproduces the observed Stokes profiles. This merit function is chosen to be the standard χ^2 -function (least square method). The minimization algorithm tries to find the value of the model's parameters that lead to synthetic Stokes profiles in closest agreement with the observed ones (i.e., to those that imply the smallest value of the merit function). The model's parameters are the magnetic field vector \mathbf{B} , the thermal velocity v_{th} , the macroscopic velocity v_{mac} and the damping of the line a . If radiative transfer effects are taken into account, this set is augmented with the optical depth of the slab ($\Delta\tau$).

The standard Levenberg-Marquardt (LM) procedure for the minimization of the χ^2 function has been used. The LM method is one of the fastest and simplest available methods when the initial estimation of the parameters is close

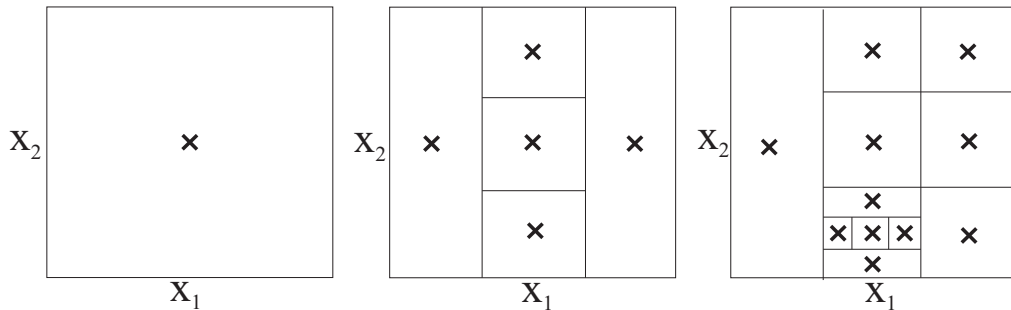


Figure 1. This figure illustrates the philosophy of the DIRECT method for searching for the region where the global minimum is located. In this case, we illustrate a case in two dimensions. After the evaluation of the function at some selected points inside each region, the DIRECT algorithm decides, using the Lipschitz condition, which rectangles can be further subdivided because they are potentially interesting. The method rapidly locates the region where the minimum is located.

to the correct minimum. On the contrary, like with the majority of the standard numerical methods for function minimization, its main drawback is that it can easily get trapped in a local minimum of the χ^2 function. A straightforward but time consuming strategy to overcome this difficulty is to restart the minimization process with different values of the initial parameters.

In our case, this difficulty has been overcome by using global optimization methods (GOM) that provide a good starting point. The majority of this type of methods are based on stochastic optimization techniques. The key idea is to efficiently sample the whole space of parameters to find the global minimum of a given function. One of the most promising methods is genetic optimization. In spite of the lack of a convergence theorem, they perform quite well in practice (e.g., Lagg et al. 2004). In our case, we propose to apply instead the DIRECT deterministic method that relies on a strong mathematical basis. The name stands for “DIviding RECTangles” (Jones et al. 1993) and the idea is to recursively sample parts of the space of parameters, locating in each iteration the part of the space where the global minimum is potentially located. The decision algorithm is based on the assumption that the function is Lipschitz continuous. For clarifying purposes, consider the case of a one-dimensional function $f : M \rightarrow R$. It is said to be Lipschitz continuous with constant α in an interval $M = [a, b]$ if:

$$|f(x) - f(x')| \leq \alpha |x - x'|, \quad \forall x, x' \in M. \quad (1)$$

In particular, a consequence of the previous equation is that the two following equations have to be fulfilled $\forall x \in M$:

$$f(x) \geq f(a) - \alpha(x - a) \quad (2)$$

$$f(x) \geq f(b) + \alpha(x - b). \quad (3)$$

These two straight lines form a V-shape below the function $f(x)$ whose intersection provides a first estimation x_1 of the minimum of the function. Repetition of this procedure in the two new subintervals $[a, x_1]$ and $[x_1, b]$ leads to new estimations x_i that converge to the global minimum. Severe problems arise when

Step	Method	Free parameters	Stokes profiles
1	DIRECT	$v_{\text{th}}, v_{\text{mac}}, \Delta\tau, a$	I
2	LM	$v_{\text{th}}, v_{\text{mac}}, \Delta\tau, a$	I
3	DIRECT	B, θ_B, χ_B	I, Q, U, V
4	LM	B, θ_B, χ_B	I, Q, U, V

Table 1. Scheme applied for the inversion of the Stokes profiles. The two DIRECT cycles are used for obtaining an initial value of the parameters as close to the global minimum as possible. This is accomplished by the fast global convergence of DIRECT. Then, a few LM iterations are sufficient to rapidly refine the value of the minimum.

generalizing this method to higher dimensions because of the difficulty in estimating the Lipschitz constant. Actually, the function is often not Lipschitz continuous. The DIRECT algorithm overcomes these problems because it does not require knowledge of the Lipschitz constant. It uses all possible values of such a constant to determine if a region of the space of parameters should be broken into subregions because of its potential interest. Fig. 1 shows a schematic illustration of the subdivision process for a function of two parameters.

One of the main drawbacks of deterministic global optimization methods is that they present a very good global convergence but a poor local convergence. Therefore, they quickly locate the region of the space of parameters where the global minimum is located, but the refinement of this solution takes a very long time. Consequently, the DIRECT method is a perfect candidate for its application as an estimator of the initial value of the parameters that are then rapidly refined by the LM algorithm. Since the initial point is very close to the minimum, the LM method, thanks to the quadratic convergence behavior, takes a few iterations to rapidly converge towards the global minimum. We have confirmed that this scheme reduces the number of evaluations of the merit function. It is important to point out that, because the most time-consuming part of the optimization procedure is the evaluation of the complex forward problem (with the solution of the statistical equilibrium equations and the radiative transfer), it is fundamental to minimize the number of merit function evaluations.

A critical and fundamental point in the optimization of functions is the stopping criterion. In the few (unrealistic) cases where the value of the function at the global minimum is known (noise-free cases), it is possible to stop the convergence process when the relative error is smaller than a fixed value. In the general case with DIRECT, very good results are obtained when the hypervolume (in the parameter space) where the algorithm is looking for the global minimum has been reduced by a given factor, $f \approx 0.001$, with respect to the original hypervolume. Another possible option is to stop after a fixed number of evaluations of the merit function.

The full inversion scheme, shown schematically in Table 1, is started with the DIRECT method to obtain a first estimation of the thermodynamical parameters by using only Stokes I . After this initialization, some iterations of the LM method are carried out to refine the initial values of the thermodynamical parameters obtained in the previous step. Once the LM method has converged,

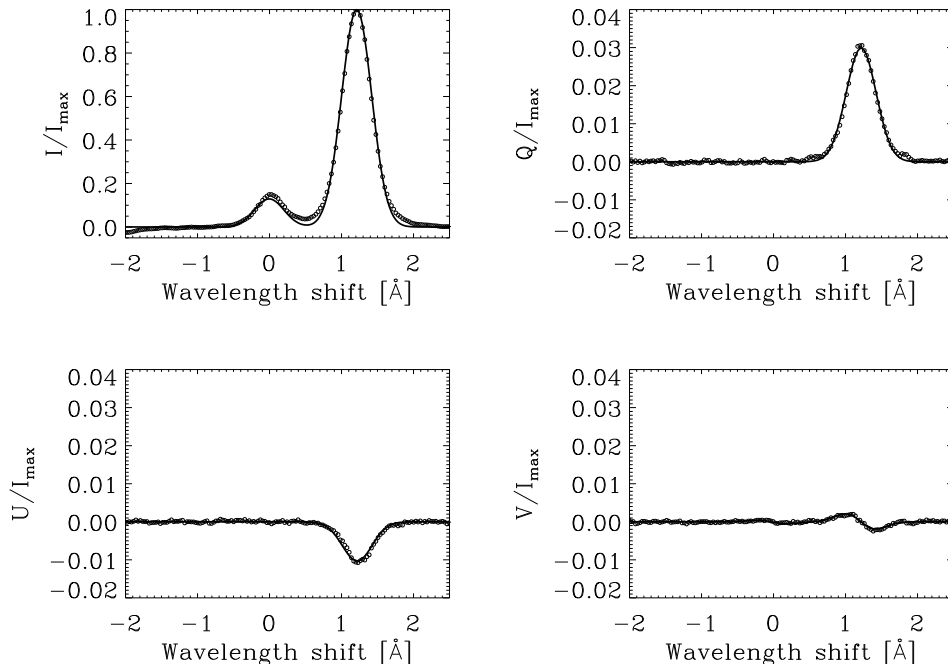


Figure 2. Example of the best theoretical fit obtained with the inversion code to the observed profiles presented in Merenda et al. (2006). The emergent Stokes profiles have been obtained by assuming an optically thin plasma. The inferred magnetic field vector is given by $B = 26.8$ G, $\theta_B = 25.5^\circ$ and $\chi_B = 161^\circ$. Furthermore, the inferred thermal velocity is $v_{th} = 7.97$ km s $^{-1}$. All these values are in close agreement with the results obtained by Merenda et al. (2006). The positive direction of Stokes Q is the one parallel to the solar limb.

the inferred values of v_{th} , v_{mac} , and a (and $\Delta\tau$ when it applies) are kept fixed. In a next step, the DIRECT method is used again for the initialization of the magnetic field vector (B , θ_B and χ_B). According to our experience, the first estimation of the magnetic field vector given by the DIRECT algorithm is typically very close to the final solution. As a final step, some iterations of the LM method are performed to refine the value of the magnetic field strength, inclination and azimuth until reaching the global optimum. Obviously, if any parameter is known in advance, we can keep it fixed during the whole inversion process.

4. Illustrative Applications

Here we have only space to demonstrate the application of this new plasma diagnostic tool to the case of a prominence and to that of an emerging magnetic flux region. For more details and applications see Asensio Ramos & Trujillo Bueno (in preparation).

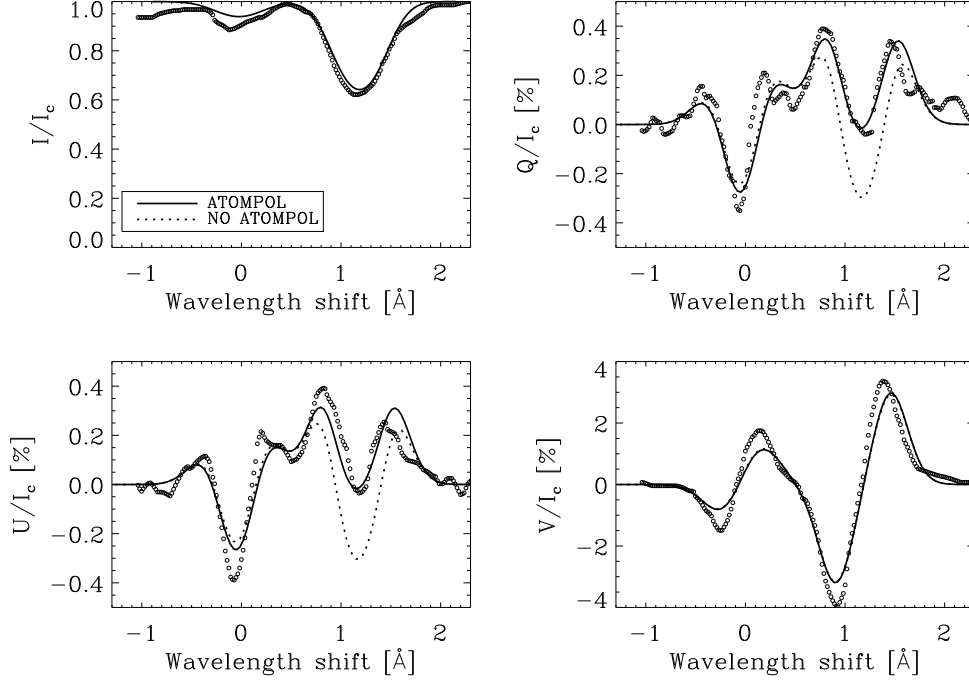


Figure 3. Emergent Stokes profiles of the HeI 10830 Å multiplet in an emerging flux region. The circles represent the observations shown by Lagg et al. (2004) in their Fig. 2. The dotted lines present the best theoretical fit obtained neglecting the influence of atomic level polarization, which corresponds to $B = 1070$ G, $\theta_B = 86^\circ$ and $\chi_B = -160^\circ$. On the contrary, the solid lines show the best fit when the effect of atomic level polarization is included, giving $B = 1009$ G, $\theta_B = 91^\circ$ and $\chi_B = -161^\circ$. The best fit to the observations is provided by the solid lines, which indicates the presence of atomic level polarization in a relatively strong field region.

4.1. A polar crown prominence

For illustrative purposes, we have applied our inversion code to infer the magnetic field vector of the polar crown prominence that generated the Stokes profiles presented in Fig. 9 of Merenda et al. (2006). We have assumed that the prominence plasma was optically thin. Our inversion code was used to infer the value of the thermal velocity v_{th} and the magnetic field vector (B, θ_B, χ_B) . The height of the prominence atoms was fixed at $h = 20''$, the same value used by Merenda et al. (2006). After the four steps summarized in Table 1, we ended up with a thermal velocity of $v_{th} = 7.97$ km s $^{-1}$ and a magnetic field vector characterized by $B = 26.8$ G, $\theta_B = 25.5^\circ$, and $\chi_B = 161.0^\circ$. The inferred magnetic field vector is in very good agreement with that obtained by Merenda et al. (2006), namely $B = 26$ G, $\theta_B = 25^\circ$, and $\chi_B = 160.5^\circ$. Therefore, we fully support their conclusion of nearly-vertical fields in the observed polar-crown prominence.

4.2. An emerging Magnetic flux region

As pointed out by Trujillo Bueno & Asensio Ramos (2007), the modeling of the emergent Stokes Q and U profiles of the He I 10830 Å multiplet should be done by taking into account the possible presence of atomic level polarization, even for magnetic field strengths as large as 1000 G. An example of a spectropolarimetric observation of an emerging magnetic flux region is shown by the circles of Fig. 3. The solid lines show the best theoretical fit to these observations of Lagg et al. (2004). Here, in addition to the Zeeman effect, we took into account the influence of atomic level polarization. The dotted lines neglect the atomic level polarization that is induced by anisotropic radiation pumping in the solar atmosphere. Our results indicate the presence of atomic level polarization in a relatively strong field region (~ 1000 G). However, it may be tranquilizing to point out that both inversions of the observed profiles yield a similar magnetic field vector, in spite of the fact that the corresponding theoretical fit is much better for the case that includes atomic level polarization.

Acknowledgments. We would like to thank Egidio Landi Degl’Innocenti for sharing with us his deep knowledge on the physics of spectral line polarization. This research has been funded by the Spanish Ministerio de Educación y Ciencia through project AYA2004-05792.

References

- Bommier V., 1977, Thèse de 3ème Cycle, Université de Paris VI
 Centeno R., Collados M., Trujillo Bueno J., 2006, *ApJ* 640, 1153
 Condon E. U., Shortley G. H., 1935, *The Theory of Atomic Spectra*, Cambridge University Press, Cambridge
 Harvey J., Hall D., 1971, in R. Howard (ed.), *IAU Symp. 43: Solar Magnetic Fields*, 279
 Jones D. R., Perttunen C. D., Stuckmann B. E., 1993, *Journal of Optimization Theory and Applications* 79, 157
 Lagg A., Woch J., Krupp N., Solanki S. K., 2004, *A&A* 414, 1109
 Landi Degl’Innocenti E., 1982, *Solar Phys.* 79, 291
 Landi Degl’Innocenti E., Landolfi M., 2004, *Polarization in Spectral Lines*, Kluwer, Dordrecht
 Lin H., Penn M. J., Kuhn J. R., 1998, *ApJ* 493, 978
 Merenda L., Trujillo Bueno J., Landi Degl’Innocenti E., Collados M., 2006, *ApJ* 642, 554
 Pierce K., 2000, in *Allen’s Astrophysical Quantities*, ed. A. N. Cox, Springer Verlag and AIP Press, New York
 Rüedi I., Solanki S. K., Livingston W., Harvey J., 1995, *A&AS* 113, 91
 Socas-Navarro H., Trujillo Bueno J., Landi Degl’Innocenti E., 2004, *ApJ* 612, 1175
 Solanki S. K., Lagg A., Woch J., Krupp N., Collados M., 2003, *Nat* 425, 692
 Trujillo Bueno J., 2003, in I. Hubeny, D. Mihalas, K. Werner (eds.), *Stellar Atmosphere Modeling*, ASP Conf. Ser. 288, 551
 Trujillo Bueno J., 2007, in R. Ramelli, O. Shalabiea, I. M. Saleh, J. O. Stenflo (eds.), *Int. Symp. on Solar Physics and Solar Eclipses*, Sebha University Publ., Sebha, Libya, 77
 Trujillo Bueno J., Asensio Ramos A., 2007, *ApJ* 655, 642
 Trujillo Bueno J., Landi degl’Innocenti E., Collados M., Merenda L., Manso Sainz R., 2002, *Nat* 415, 403
 Trujillo Bueno J., Merenda L., Centeno R., Collados M., Landi Degl’Innocenti E., 2005, *ApJ* 619, L191